

A radial basis functions solution for the analysis of laminated doubly-curved shells by a Reissner-Mixed Variational Theorem

Original

A radial basis functions solution for the analysis of laminated doubly-curved shells by a Reissner-Mixed Variational Theorem / Ferreira, A. J. M.; Carrera, Erasmo; Cinefra, Maria; Zenkour, A. M.. - In: MECHANICS OF ADVANCED MATERIALS AND STRUCTURES. - ISSN 1537-6532. - 23:9(2016), pp. 1068-1079. [10.1080/15376494.2015.1121557]

Availability:

This version is available at: 11583/2573138 since: 2016-09-23T12:32:59Z

Publisher:

Taylor & Francis

Published

DOI:10.1080/15376494.2015.1121557

Terms of use:

This article is made available under terms and conditions as specified in the corresponding bibliographic description in the repository

Publisher copyright

(Article begins on next page)

A radial basis functions solution for the analysis of laminated doubly-curved shells by a Reissner-Mixed Variational Theorem

A.J.M. Ferreira ^{a,c}, E. Carrera ^{b,c}, M. Cinefra ^b, A. M. Zenkour ^{c,d},

^a*Faculdade de Engenharia da Universidade do Porto, Porto, Portugal*

^b*Department of Aeronautics and Aerospace Engineering, Politecnico di Torino, Torino, Italy*

^c*Department of Mathematics, Faculty of Science, King Abdulaziz University, Jeddah, Saudi Arabia*

^d*Department of Mathematics, Faculty of Science, Kafrelsheikh University, Kafr El-Sheikh, Egypt.*

Abstract

In this paper, the static and free vibration analysis of doubly-curved laminated shells is performed by radial basis functions collocation. The Reissner-Mixed Variational Theorem (RMVT) via a Unified Formulation by Carrera is applied in order to obtain the equations of motion and the natural boundary conditions. The present theory accounts for through-the-thickness deformation, and directly computes displacements and transverse stresses in each interface of the laminate.

1 Introduction

Examples of multilayered shell structures used in modern industrial applications are laminated constructions, or sandwich panels.

Exhaustive overviews on classical and refined models for the analysis of multilayered structures have been reported in many published review articles. These include the papers by Grigolyuk and Kulikov [1], Kapania and Raciti [2], Kapania [3], Noor et al. [4–6], Correia et al. [8], Neves et al. [9] and Soldatos and Timarci [7]. Among the refined theories a convenient distinction can be made between models in which the number of the unknown variables is independent or dependent on the number of the constitutive layers of the shell. Following Reddy [10], we assign the name ESLM (Equivalent Single Layer Models) to the first grouping while LWM (Layer Wise Model) is used to denote the

others. Early [11–14] and more recent [15–20] LWMs have shown the superiority of layer-wise approaches over ESL approaches to predict accurately static and dynamic response of thick and very thick structures. On the other hand, LWMs are computationally expensive and the use of ESLMs is preferred in most practical applications.

In the most general cases, the finite element method is used for the analysis of shell structures and some reviews on finite element shell formulations can be found in the work by Dennis and Palazotto [21], Merk [22], and Di and Ramm [23]. In this paper, however, we use collocation with radial basis functions, with the so-called unsymmetrical Kansa method [24]. The use of radial basis function for the analysis of structures and materials has been previously studied by numerous authors [25–39]. The authors have recently applied the RBF collocation to the static deformations of composite beams and plates [40–42].

In this paper, we propose to use the Unified Formulation (UF) by Carrera [43] to derive the equations of motion and boundary conditions to analyze laminated shells, according to a layerwise-based shear deformation theory that accounts for through-the-thickness deformations. The UF is a compact formulation that permits to analyze the bi-dimensional structures irrespective of the shear deformation theory being considered and it has been applied in several finite element analysis, either using the Principle of Virtual Displacements, or by using the Reissner’s Mixed Variational Theorem (RMVT) [44–47] (which is adopted in this paper). The Unified Formulation (here referred as CUF-Carrera’s Unified Formulation) may consider both equivalent single layer theories (ESL), or layerwise theories (LW), using the Principle of Virtual Displacements (PVD). However, a more interesting (at a higher computational cost) approach is to use the layerwise formulation with the Reissner’s Variational Mixed Theorem (RMVT). The RMVT considers two independent fields for displacement and transverse stress variables. As a result, a priori interlaminar continuous transverse shear and normal stress fields can be achieved, which is quite important for sandwich-like structures. Details on the RMVT can be found in Carrera [48,50].

The analysis of laminated shells with RMVT has been implemented successfully with finite elements, but never with collocation with radial basis functions. Therefore, this paper serves to fill the gap of knowledge in this research area.

2 Unified Formulation for the Layerwise theory

In this section, it is shown how the Carrera’s Unified formulation can be used to obtain the fundamental nuclei, which allows the derivation of the

equations of motion and boundary conditions, in strong form for the present RBF collocation.

In the case of Layer Wise (LW) models, each layer k of the given multi-layered structure is separately considered. According to the CUF, the three displacement components u , v and w , along the curvilinear coordinates α , β and z , and their virtual variations can be modelled as:

$$(u^k, v^k, w^k) = F_\tau^k (u_\tau^k, v_\tau^k, w_\tau^k) \quad (\delta u^k, \delta v^k, \delta w^k) = F_s^k (\delta u_s^k, \delta v_s^k, \delta w_s^k) \quad (1)$$

where F_τ and F_s are the so-called thickness functions. τ and s are summation indexes and k indicates the layer of the multilayered structure. In the present layer-wise formulation, we choose:

$$F_\tau^k = F_s^k = [F_b^k \ F_t^k] = \left[\frac{1 - 2/h_k \left(z - \frac{1}{2} (z_k + z_{k+1}) \right)}{2} \quad \frac{1 + 2/h_k \left(z - \frac{1}{2} (z_k + z_{k+1}) \right)}{2} \right]$$

Therefore, $\tau = s = b, t$ and the polynomial order of the expansion is $N = 1$. Note that z_k, z_{k+1} correspond to the bottom and top z -coordinates for each layer k .

In a similar way, the transverse shear/normal stresses $\boldsymbol{\sigma}_n = (\sigma_{\alpha z}, \sigma_{\beta z}, \sigma_{zz})$ can also be modelled as

$$\boldsymbol{\sigma}_n^k = F_b \boldsymbol{\sigma}_{nt}^k + F_t \boldsymbol{\sigma}_{nb}^k = F_\tau \boldsymbol{\sigma}_\tau^k \quad (2)$$

The same expansion is used for the virtual variation of transverse stresses by considering the index s . We then obtain all terms of the equations of motion by integrating through the thickness direction.

2.1 Doubly-curved shells

Shells are bi-dimensional structures in which one dimension (in general the thickness in z direction) is negligible with respect to the other two in-plane dimensions. The geometry and the reference system of a doubly-curved shell are indicated in the Figures 1 and 2. Considering this geometry, the square of an infinitesimal linear segment in the layer ds_k , the associated infinitesimal

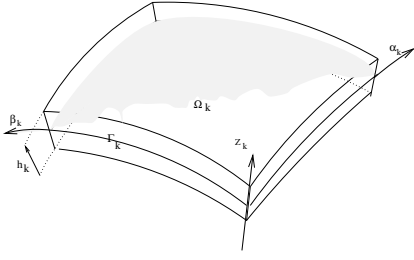


Fig. 1. Curvilinear reference system.

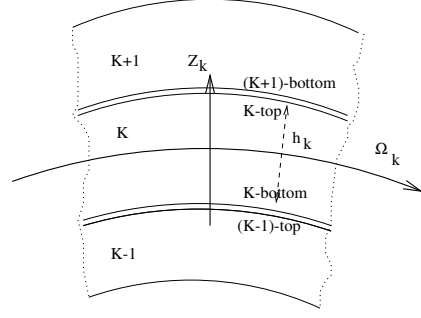


Fig. 2. Through-the-thickness reference system.

area $d\Omega_k$ and volume dV_k are given by:

$$ds_k^2 = H_\alpha^{k^2} d\alpha^2 + H_\beta^{k^2} d\beta^2 + H_z^{k^2} dz^2 ,$$

$$d\Omega_k = H_\alpha^k H_\beta^k d\alpha d\beta , \quad (3)$$

$$dV_k = H_\alpha^k H_\beta^k H_z^k d\alpha d\beta dz ,$$

where the metric coefficients are:

$$H_\alpha^k = A^k(1 + z/R_\alpha^k), \quad H_\beta^k = B^k(1 + z/R_\beta^k), \quad H_z^k = 1 . \quad (4)$$

R_α^k and R_β^k are the principal radii of curvature along the orthogonal curvilinear coordinates α and β , respectively. While, A^k and B^k are the Lamé parameters, Ω_k is the domain of the shell surface and Γ_k is the boundary of Ω_k . For more details about the description of the geometry in doubly-curved shells, the readers can refer to the work by Leissa [51]. In this work, the attention has been restricted to shells with constant radii of curvature (in particular, spherical shells) for which $A^k = B^k = 1$.

3 Strains and stresses

Strains and stresses are separated into in-plane and normal components, denoted respectively by the subscripts p and n .

In doubly-curved shells with $A^k = B^k = 1$, the mechanical strains in the k th layer can be related to the displacement field $\mathbf{u}^k = \{u^k, v^k, w^k\}$ via the geometrical relations presented in [52], that are:

$$\epsilon_{pG}^k = [\epsilon_{\alpha\alpha}^k, \epsilon_{\beta\beta}^k, \epsilon_{\alpha\beta}^k]^T = (\mathbf{D}_p^k + \mathbf{A}_p^k) \mathbf{u}^k, \quad \epsilon_{nG}^k = [\epsilon_{\alpha z}^k, \epsilon_{\beta z}^k, \epsilon_{zz}^k]^T = (\mathbf{D}_{nz}^k + \mathbf{D}_{nz}^k - \mathbf{A}_n^k) \mathbf{u}^k \quad (5)$$

The explicit form of the introduced arrays is:

$$\mathbf{D}_p^k = \begin{bmatrix} \frac{\partial_\alpha}{H_\alpha^k} & 0 & 0 \\ 0 & \frac{\partial_\beta}{H_\beta^k} & 0 \\ \frac{\partial_\beta}{H_\beta^k} & \frac{\partial_\alpha}{H_\alpha^k} & 0 \end{bmatrix}, \quad \mathbf{D}_{n\Omega}^k = \begin{bmatrix} 0 & 0 & \frac{\partial_\alpha}{H_\alpha^k} \\ 0 & 0 & \frac{\partial_\beta}{H_\beta^k} \\ 0 & 0 & 0 \end{bmatrix}, \quad \mathbf{D}_{nz}^k = \begin{bmatrix} \partial_z & 0 & 0 \\ 0 & \partial_z & 0 \\ 0 & 0 & \partial_z \end{bmatrix}, \quad (6)$$

$$\mathbf{A}_p^k = \begin{bmatrix} 0 & 0 & \frac{1}{H_\alpha^k R_\alpha^k} \\ 0 & 0 & \frac{1}{H_\beta^k R_\beta^k} \\ 0 & 0 & 0 \end{bmatrix}, \quad \mathbf{A}_n^k = \begin{bmatrix} \frac{1}{H_\alpha^k R_\alpha^k} & 0 & 0 \\ 0 & \frac{1}{H_\beta^k R_\beta^k} & 0 \\ 0 & 0 & 0 \end{bmatrix}. \quad (7)$$

where ∂ indicates the partial derivation.

The stresses are expressed by means of the constitutive relations. For a classical model, they state:

$$\begin{aligned} \boldsymbol{\sigma}_p^k &= \mathbf{C}_{pp}^k \boldsymbol{\epsilon}_p^k + \mathbf{C}_{pn}^k \boldsymbol{\epsilon}_n^k \\ \boldsymbol{\sigma}_n^k &= \mathbf{C}_{np}^k \boldsymbol{\epsilon}_p^k + \mathbf{C}_{nn}^k \boldsymbol{\epsilon}_n^k \end{aligned} \quad (8)$$

where the material matrices are:

$$\begin{aligned} \mathbf{C}_{pp}^k &= \begin{bmatrix} C_{11} & C_{12} & C_{16} \\ C_{12} & C_{22} & C_{26} \\ C_{16} & C_{26} & C_{66} \end{bmatrix} & \mathbf{C}_{pn}^k &= \begin{bmatrix} 0 & 0 & C_{13} \\ 0 & 0 & C_{23} \\ 0 & 0 & C_{36} \end{bmatrix} \\ \mathbf{C}_{np}^k &= \mathbf{C}_{pn}^{kT}; & \mathbf{C}_{nn}^k &= \begin{bmatrix} C_{44} & C_{45} & 0 \\ C_{45} & C_{55} & 0 \\ 0 & 0 & C_{33} \end{bmatrix} \end{aligned} \quad (9)$$

In the case of mixed models, the displacements \mathbf{u} and the transverse shear/normal stresses $\boldsymbol{\sigma}_n$ are both a priori variables. From the second equation of (8), one obtains:

$$\boldsymbol{\epsilon}_n^k = -(\mathbf{C}_{nn}^k)^{-1} \mathbf{C}_{np}^k \boldsymbol{\epsilon}_p^k + (\mathbf{C}_{nn}^k)^{-1} \boldsymbol{\sigma}_n^k \quad (10)$$

After substitution into the first equation of (8), the constitutive equations are rewritten as follows:

$$\begin{aligned} \boldsymbol{\sigma}_p^k &= \tilde{\mathbf{C}}_{pp}^k(z) \boldsymbol{\epsilon}_p^k + \tilde{\mathbf{C}}_{pn}^k(z) \boldsymbol{\sigma}_n^k \\ \boldsymbol{\epsilon}_n^k &= \tilde{\mathbf{C}}_{np}^k(z) \boldsymbol{\epsilon}_p^k + \tilde{\mathbf{C}}_{nn}^k(z) \boldsymbol{\sigma}_n^k \end{aligned} \quad (11)$$

where the new coefficients are:

$$\begin{aligned}\tilde{C}_{pp}^k &= C_{pp}^k - C_{pn}^k C_{nn}^{k-1} C_{np}^k & \tilde{C}_{pn}^k &= C_{pn}^k C_{nn}^{k-1} \\ \tilde{C}_{np}^k &= -C_{nn}^{k-1} C_{np}^k & \tilde{C}_{nn}^k &= C_{nn}^{k-1}\end{aligned}\quad (12)$$

For further details about the explicit expression of the material constants C_{ij} , one can refer to [19] and [20].

4 Governing equations by RMVT

In the case of doubly-curved shell geometry, the Reissner's Mixed Variational Theorem takes into account the metric coefficients H_α and H_β , given in equation (4):

$$\sum_{k=1}^{N_l} \int_{\Omega_k} \int_{A_k} \left\{ \delta \epsilon_{pG}^k{}^T \sigma_{pC}^k + \delta \epsilon_{nG}^k{}^T \sigma_{nM}^k + \delta \sigma_{nM}^k{}^T (\epsilon_{nG}^k - \epsilon_{nC}^k) \right\} H_\alpha H_\beta d\Omega_k dz = \sum_{k=1}^{N_l} \delta L_e^k \quad (13)$$

where N_l is the number of layers, A_k is the integration domain along the thickness and L_e^k is the work done by the external loads. The meaning of the subscripts is: M = modelled a-priori, G = derived from geometrical relations and C = obtained via the constitutive equations. Substituting the geometrical relations for the shell (5), the constitutive equations (11) and the CUF for both the displacement components (1) and the transverse stresses (2), and then performing the integration by parts, the governing equations in the case of RMVT are:

$$\begin{aligned}\delta \mathbf{u}_s^k{}^T : & \quad \mathbf{K}_{uu}^{k\tau s} \mathbf{u}_\tau^k + \mathbf{K}_{u\sigma}^{k\tau s} \boldsymbol{\sigma}_{n\tau}^k = \mathbf{P}_{u\tau}^k \\ \delta \boldsymbol{\sigma}_{ns}^k{}^T : & \quad \mathbf{K}_{\sigma u}^{k\tau s} \mathbf{u}_\tau^k + \mathbf{K}_{\sigma\sigma}^{k\tau s} \boldsymbol{\sigma}_{n\tau}^k = 0\end{aligned}\quad (14)$$

with the following boundary conditions:

$$\boldsymbol{\Pi}_u^{k\tau s} \mathbf{u}_\tau^k + \boldsymbol{\Pi}_\sigma^{k\tau s} \boldsymbol{\sigma}_{n\tau}^k = \boldsymbol{\Pi}_u^{k\tau s} \bar{\mathbf{u}}_\tau^k + \boldsymbol{\Pi}_\sigma^{k\tau s} \bar{\boldsymbol{\sigma}}_{n\tau}^k \quad (15)$$

The arrays introduced (the so-called fundamental nuclei) are described in detail in the following section.

4.1 Fundamental nuclei

The following integrals are introduced to perform the explicit form of fundamental nuclei:

$$\begin{aligned}
(J^{k\tau s}, J_{\alpha}^{k\tau s}, J_{\beta}^{k\tau s}, J_{\frac{\alpha}{\beta}}^{k\tau s}, J_{\frac{\beta}{\alpha}}^{k\tau s}, J_{\alpha\beta}^{k\tau s}) &= \int_{A_k} F_{\tau} F_s (1, H_{\alpha}, H_{\beta}, \frac{H_{\alpha}}{H_{\beta}}, \frac{H_{\beta}}{H_{\alpha}}, H_{\alpha} H_{\beta}) dz \\
(J^{k\tau z s}, J_{\alpha}^{k\tau z s}, J_{\beta}^{k\tau z s}, J_{\frac{\alpha}{\beta}}^{k\tau z s}, J_{\frac{\beta}{\alpha}}^{k\tau z s}, J_{\alpha\beta}^{k\tau z s}) &= \int_{A_k} \frac{\partial F_{\tau}}{\partial z} F_s (1, H_{\alpha}, H_{\beta}, \frac{H_{\alpha}}{H_{\beta}}, \frac{H_{\beta}}{H_{\alpha}}, H_{\alpha} H_{\beta}) dz \\
(J^{k\tau s z}, J_{\alpha}^{k\tau s z}, J_{\beta}^{k\tau s z}, J_{\frac{\alpha}{\beta}}^{k\tau s z}, J_{\frac{\beta}{\alpha}}^{k\tau s z}, J_{\alpha\beta}^{k\tau s z}) &= \int_{A_k} F_{\tau} \frac{\partial F_s}{\partial z} (1, H_{\alpha}, H_{\beta}, \frac{H_{\alpha}}{H_{\beta}}, \frac{H_{\beta}}{H_{\alpha}}, H_{\alpha} H_{\beta}) dz \\
(J^{k\tau z s z}, J_{\alpha}^{k\tau z s z}, J_{\beta}^{k\tau z s z}, J_{\frac{\alpha}{\beta}}^{k\tau z s z}, J_{\frac{\beta}{\alpha}}^{k\tau z s z}, J_{\alpha\beta}^{k\tau z s z}) &= \int_{A_k} \frac{\partial F_{\tau}}{\partial z} \frac{\partial F_s}{\partial z} (1, H_{\alpha}, H_{\beta}, \frac{H_{\alpha}}{H_{\beta}}, \frac{H_{\beta}}{H_{\alpha}}, H_{\alpha} H_{\beta}) dz
\end{aligned} \tag{16}$$

The expression of fundamental nuclei for the left-hand side is expressed as:

$$\mathbf{K}^{k\tau s} = \begin{bmatrix} \mathbf{K}_{uu}^{k\tau s} & \mathbf{K}_{u\sigma}^{k\tau s} \\ \mathbf{K}_{\sigma u}^{k\tau s} & \mathbf{K}_{\sigma\sigma}^{k\tau s} \end{bmatrix} \tag{17}$$

where

$$\mathbf{K}_{uu}^{k\tau s} = \int_{A_k} \left[[-\mathbf{D}_p + \mathbf{A}_p]^T \tilde{\mathbf{C}}_{pp}^k [\mathbf{D}_p + \mathbf{A}_p] \right] F_s F_{\tau} H_{\alpha} H_{\beta} dz, \tag{18}$$

$$\mathbf{K}_{u\sigma}^{k\tau s} = \int_{A_k} \left[-\mathbf{D}_p + \mathbf{A}_p \right]^T \tilde{\mathbf{C}}_{pn}^k + [-\mathbf{D}_{n\Omega} + \mathbf{D}_{nz} - \mathbf{A}_n]^T \right] F_s F_{\tau} H_{\alpha} H_{\beta} dz, \tag{19}$$

$$\mathbf{K}_{\sigma u}^{k\tau s} = \int_{A_k} \left[[\mathbf{D}_{n\Omega} + \mathbf{D}_{nz} - \mathbf{A}_n] - \tilde{\mathbf{C}}_{np}^k [\mathbf{D}_p + \mathbf{A}_p] \right] F_s F_{\tau} H_{\alpha} H_{\beta} dz, \tag{20}$$

$$\mathbf{K}_{\sigma\sigma}^{k\tau s} = \int_{A_k} \left[-\tilde{\mathbf{C}}_{nn}^k \right] F_s F_{\tau} H_{\alpha} H_{\beta} dz, \tag{21}$$

and the nuclei for the boundary conditions are:

$$\mathbf{\Pi}_u^{k\tau s} = \int_{A_k} \left[\mathbf{I}_p^T \tilde{\mathbf{C}}_{pp}^k [\mathbf{D}_p + \mathbf{A}_p] \right] F_s F_{\tau} H_{\alpha} H_{\beta} dz, \tag{22}$$

$$\mathbf{\Pi}_{\sigma}^{k\tau s} = \int_{A_k} \left[\mathbf{I}_p^T \tilde{\mathbf{C}}_{pn}^k + \mathbf{I}_{n\Omega}^T \right] F_s F_{\tau} H_{\alpha} H_{\beta} dz, \tag{23}$$

Using the notation given in equations (16), the nuclei components $\mathbf{K}_{uu}^{k\tau s}$ in explicit form are given as:

$$\mathbf{K}_{uu}^{k\tau s} = \begin{bmatrix} K_{uu11}^{k\tau s} & K_{uu12}^{k\tau s} & K_{uu13}^{k\tau s} \\ K_{uu21}^{k\tau s} & K_{uu22}^{k\tau s} & K_{uu23}^{k\tau s} \\ K_{uu31}^{k\tau s} & K_{uu32}^{k\tau s} & K_{uu33}^{k\tau s} \end{bmatrix} \quad (24)$$

where

$$\begin{aligned} K_{uu11}^{k\tau s} = & -\partial_\alpha^\tau \partial_\alpha^s C_{11}^k J_{\beta/\alpha}^{k\tau s} - \partial_\alpha^\tau \partial_\beta^s C_{16}^k J^{k\tau s} - \partial_\beta^\tau \partial_\alpha^s C_{16}^k J^{k\tau s} + \partial_\alpha^\tau \partial_\alpha^s \frac{C_{13}^{k^2}}{C_{33}^k} J_{\beta/\alpha}^{k\tau s} + \\ & \partial_\alpha^\tau \partial_\beta^s \frac{C_{13}^k C_{36}^k}{C_{33}^k} J^{k\tau s} + \partial_\beta^\tau \partial_\alpha^s \frac{C_{13}^k C_{36}^k}{C_{33}^k} J^{k\tau s} + \partial_\beta^\tau \partial_\beta^s \frac{C_{36}^{k^2}}{C_{33}^k} J_{\alpha/\beta}^{k\tau s} - \partial_\beta^\tau \partial_\beta^s C_{66}^k J_{\alpha/\beta}^{k\tau s} \end{aligned} \quad (25)$$

$$\begin{aligned} K_{uu12}^{k\tau s} = & -\partial_\alpha^\tau \partial_\beta^s C_{12}^k J^{k\tau s} - \partial_\alpha^\tau \partial_\alpha^s C_{16}^k J_{\beta/\alpha}^{k\tau s} - \partial_\beta^\tau \partial_\beta^s C_{26}^k J_{\alpha/\beta}^{k\tau s} + \partial_\alpha^\tau \partial_\beta^s \frac{C_{13}^k C_{23}^k}{C_{33}^k} J^{k\tau s} + \\ & \partial_\alpha^\tau \partial_\alpha^s \frac{C_{13}^k C_{36}^k}{C_{33}^k} J_{\beta/\alpha}^{k\tau s} + \partial_\beta^\tau \partial_\beta^s \frac{C_{23}^k C_{36}^k}{C_{33}^k} J_{\alpha/\beta}^{k\tau s} + \partial_\beta^\tau \partial_\alpha^s \frac{C_{36}^{k^2}}{C_{33}^k} J^{k\tau s} - \partial_\beta^\tau \partial_\alpha^s C_{66}^k J^{k\tau s} \end{aligned} \quad (26)$$

$$\begin{aligned} K_{uu13}^{k\tau s} = & -\frac{1}{R_\alpha^k} \partial_\beta^\tau C_{16}^k J^{k\tau s} - \frac{1}{R_\beta^k} \partial_\beta^\tau C_{26}^k J_{\alpha/\beta}^{k\tau s} + \frac{1}{R_\alpha^k} \partial_\beta^\tau \frac{C_{13}^k C_{36}^k}{C_{33}^k} J^{k\tau s} + \frac{1}{R_\beta^k} \partial_\beta^\tau \frac{C_{23}^k C_{36}^k}{C_{33}^k} J_{\alpha/\beta}^{k\tau s} - \\ & \frac{1}{R_\alpha^k} \partial_\alpha^\tau C_{11}^k J_{\beta/\alpha}^{k\tau s} - \frac{1}{R_\beta^k} \partial_\alpha^\tau C_{12}^k J^{k\tau s} + \frac{1}{R_\alpha^k} \partial_\alpha^\tau \frac{C_{13}^{k^2}}{C_{33}^k} J_{\beta/\alpha}^{k\tau s} + \frac{1}{R_\beta^k} \partial_\alpha^\tau \frac{C_{13}^k C_{23}^k}{C_{33}^k} J^{k\tau s} \end{aligned} \quad (27)$$

$$\begin{aligned} K_{uu21}^{k\tau s} = & -\partial_\beta^\tau \partial_\alpha^s C_{12}^k J^{k\tau s} - \partial_\alpha^\tau \partial_\alpha^s C_{16}^k J_{\beta/\alpha}^{k\tau s} - \partial_\beta^\tau \partial_\beta^s C_{26}^k J_{\alpha/\beta}^{k\tau s} + \partial_\beta^\tau \partial_\alpha^s \frac{C_{13}^k C_{23}^k}{C_{33}^k} J^{k\tau s} + \\ & \partial_\alpha^\tau \partial_\alpha^s \frac{C_{13}^k C_{36}^k}{C_{33}^k} J_{\beta/\alpha}^{k\tau s} + \partial_\beta^\tau \partial_\beta^s \frac{C_{23}^k C_{36}^k}{C_{33}^k} J_{\alpha/\beta}^{k\tau s} + \partial_\alpha^\tau \partial_\beta^s \frac{C_{36}^{k^2}}{C_{33}^k} J^{k\tau s} - \partial_\alpha^\tau \partial_\beta^s C_{66}^k J^{k\tau s} \end{aligned} \quad (28)$$

$$\begin{aligned} K_{uu22}^{k\tau s} = & -\partial_\beta^\tau \partial_\beta^s C_{22}^k J_{\alpha/\beta}^{k\tau s} - \partial_\alpha^\tau \partial_\beta^s C_{26}^k J^{k\tau s} - \partial_\beta^\tau \partial_\alpha^s C_{26}^k J^{k\tau s} + \partial_\beta^\tau \partial_\beta^s \frac{C_{23}^{k^2}}{C_{33}^k} J_{\alpha/\beta}^{k\tau s} + \\ & \partial_\alpha^\tau \partial_\beta^s \frac{C_{23}^k C_{36}^k}{C_{33}^k} J^{k\tau s} + \partial_\beta^\tau \partial_\alpha^s \frac{C_{23}^k C_{36}^k}{C_{33}^k} J^{k\tau s} + \partial_\alpha^\tau \partial_\alpha^s \frac{C_{36}^{k^2}}{C_{33}^k} J_{\beta/\alpha}^{k\tau s} - \partial_\alpha^\tau \partial_\alpha^s C_{66}^k J_{\beta/\alpha}^{k\tau s} \end{aligned} \quad (29)$$

$$\begin{aligned} K_{uu23}^{k\tau s} = & -\frac{1}{R_\alpha^k} \partial_\beta^\tau C_{12}^k J^{k\tau s} - \frac{1}{R_\beta^k} \partial_\beta^\tau C_{22}^k J_{\alpha/\beta}^{k\tau s} + \frac{1}{R_\alpha^k} \partial_\beta^\tau \frac{C_{13}^k C_{23}^k}{C_{33}^k} J^{k\tau s} + \frac{1}{R_\beta^k} \partial_\beta^\tau \frac{C_{23}^{k^2}}{C_{33}^k} J_{\alpha/\beta}^{k\tau s} - \\ & \frac{1}{R_\alpha^k} \partial_\alpha^\tau C_{16}^k J_{\beta/\alpha}^{k\tau s} - \frac{1}{R_\beta^k} \partial_\alpha^\tau C_{26}^k J^{k\tau s} + \frac{1}{R_\alpha^k} \partial_\alpha^\tau \frac{C_{13}^k C_{36}^k}{C_{33}^k} J_{\beta/\alpha}^{k\tau s} + \frac{1}{R_\beta^k} \partial_\alpha^\tau \frac{C_{23}^k C_{36}^k}{C_{33}^k} J^{k\tau s} \end{aligned} \quad (30)$$

$$\begin{aligned}
K_{uu_{31}}^{k\tau s} = & \frac{1}{R_\alpha^k} \partial_\beta^s C_{16}^k J^{k\tau s} + \frac{1}{R_\beta^k} \partial_\beta^s C_{26}^k J_{\alpha/\beta}^{k\tau s} - \frac{1}{R_\alpha^k} \partial_\beta^s \frac{C_{13}^k C_{36}^k}{C_{33}^k} J^{k\tau s} - \frac{1}{R_\beta^k} \partial_\beta^s \frac{C_{23}^k C_{36}^k}{C_{33}^k} J_{\alpha/\beta}^{k\tau s} + \\
& \frac{1}{R_\alpha^k} \partial_\alpha^s C_{11}^k J_{\beta/\alpha}^{k\tau s} + \frac{1}{R_\beta^k} \partial_\alpha^s C_{12}^k J^{k\tau s} - \frac{1}{R_\alpha^k} \partial_\alpha^s \frac{C_{13}^{k^2}}{C_{33}^k} J_{\beta/\alpha}^{k\tau s} - \frac{1}{R_\beta^k} \partial_\alpha^s \frac{C_{13}^k C_{23}^k}{C_{33}^k} J^{k\tau s}
\end{aligned} \tag{31}$$

$$\begin{aligned}
K_{uu_{32}}^{k\tau s} = & \frac{1}{R_\alpha^k} \partial_\beta^s C_{12}^k J^{k\tau s} + \frac{1}{R_\beta^k} \partial_\beta^s C_{22}^k J_{\alpha/\beta}^{k\tau s} - \frac{1}{R_\alpha^k} \partial_\beta^s \frac{C_{13}^k C_{23}^k}{C_{33}^k} J^{k\tau s} - \frac{1}{R_\beta^k} \partial_\beta^s \frac{C_{23}^{k^2}}{C_{33}^k} J_{\alpha/\beta}^{k\tau s} + \\
& \frac{1}{R_\alpha^k} \partial_\alpha^s C_{16}^k J_{\beta/\alpha}^{k\tau s} + \frac{1}{R_\beta^k} \partial_\alpha^s C_{26}^k J^{k\tau s} - \frac{1}{R_\alpha^k} \partial_\alpha^s \frac{C_{13}^k C_{36}^k}{C_{33}^k} J_{\beta/\alpha}^{k\tau s} - \frac{1}{R_\beta^k} \partial_\alpha^s \frac{C_{23}^k C_{36}^k}{C_{33}^k} J^{k\tau s}
\end{aligned} \tag{32}$$

$$\begin{aligned}
K_{uu_{33}}^{k\tau s} = & \frac{1}{R_\alpha^{k^2}} C_{11}^k J_{\beta/\alpha}^{k\tau s} + \frac{2}{R_\alpha R_\beta^k} C_{12}^k J^{k\tau s} + \frac{1}{R_\beta^{k^2}} C_{22}^k J_{\alpha/\beta}^{k\tau s} - \frac{1}{R_\alpha^{k^2}} \frac{C_{13}^{k^2}}{C_{33}^k} J_{\beta/\alpha}^{k\tau s} - \\
& \frac{2}{R_\alpha^k R_\beta^k} \frac{C_{13}^k C_{23}^k}{C_{33}^k} J^{k\tau s} - \frac{1}{R_\beta^{k^2}} \frac{C_{23}^{k^2}}{C_{33}^k} J_{\alpha/\beta}^{k\tau s}
\end{aligned} \tag{33}$$

$$\mathbf{K}_{u\sigma}^{k\tau s} = \begin{bmatrix} K_{u\sigma_{11}}^{k\tau s} & K_{u\sigma_{12}}^{k\tau s} & K_{u\sigma_{13}}^{k\tau s} \\ K_{u\sigma_{21}}^{k\tau s} & K_{u\sigma_{22}}^{k\tau s} & K_{u\sigma_{23}}^{k\tau s} \\ K_{u\sigma_{31}}^{k\tau s} & K_{u\sigma_{32}}^{k\tau s} & K_{u\sigma_{33}}^{k\tau s} \end{bmatrix} = \tag{34}$$

$$\left[\begin{array}{c|c|c} -\frac{1}{R_\alpha^k} J_\beta^{k\tau s} + J_{\alpha\beta}^{k\tau, z^s} & 0 & -\partial_\alpha^\tau \frac{C_{13}^k}{C_{33}^k} J_\beta^{k\tau s} - \partial_\beta^\tau \frac{C_{36}^k}{C_{33}^k} J_\alpha^{k\tau s} \\ 0 & -\frac{1}{R_\beta^k} J_\alpha^{k\tau s} + J_{\alpha\beta}^{k\tau, z^s} & -\partial_\beta^\tau \frac{C_{23}^k}{C_{33}^k} J_\alpha^{k\tau s} - \partial_\alpha^\tau \frac{C_{36}^k}{C_{33}^k} J_\beta^{k\tau s} \\ -\partial_\alpha^\tau J_\beta^{k\tau s} & -\partial_\beta^\tau J_\alpha^{k\tau s} & J_{\alpha\beta}^{k\tau, z^s} + \frac{1}{R_\alpha^k} \frac{C_{13}^k}{C_{33}^k} J_\beta^{k\tau s} + \frac{1}{R_\beta^k} \frac{C_{23}^k}{C_{33}^k} J_\alpha^{k\tau s} \end{array} \right]$$

$$\mathbf{K}_{\sigma u}^{k\tau s} = \begin{bmatrix} K_{\sigma u_{11}}^{k\tau s} & K_{\sigma u_{12}}^{k\tau s} & K_{\sigma u_{13}}^{k\tau s} \\ K_{\sigma u_{21}}^{k\tau s} & K_{\sigma u_{22}}^{k\tau s} & K_{\sigma u_{23}}^{k\tau s} \\ K_{\sigma u_{31}}^{k\tau s} & K_{\sigma u_{32}}^{k\tau s} & K_{\sigma u_{33}}^{k\tau s} \end{bmatrix} =$$

$$\left[\begin{array}{c|c|c} -\frac{1}{R_\alpha^k} J_\beta^{k\tau s} + J_{\alpha\beta}^{k\tau, z} & 0 & \partial_\alpha^s J_\beta^{k\tau s} \\ 0 & -\frac{1}{R_\beta^k} J_\alpha^{k\tau s} + J_{\alpha\beta}^{k\tau, z} & \partial_\beta^s J_\alpha^{k\tau s} \\ \partial_\alpha^s \frac{C_{13}^k}{C_{33}^k} J_\beta^{k\tau s} + \partial_\beta^s \frac{C_{36}^k}{C_{33}^k} J_\alpha^{k\tau s} & \partial_\beta^s \frac{C_{23}^k}{C_{33}^k} J_\alpha^{k\tau s} + \partial_\alpha^s \frac{C_{36}^k}{C_{33}^k} J_\beta^{k\tau s} & J_{\alpha\beta}^{k\tau, z} + \frac{1}{R_\alpha^k} \frac{C_{13}^k}{C_{33}^k} J_\beta^{k\tau s} + \frac{1}{R_\beta^k} \frac{C_{23}^k}{C_{33}^k} J_\alpha^{k\tau s} \end{array} \right] \tag{35}$$

$$K_{\sigma\sigma}^{k\tau s} = \begin{bmatrix} K_{\sigma\sigma 11}^{k\tau s} & K_{\sigma\sigma 12}^{k\tau s} & K_{\sigma\sigma 13}^{k\tau s} \\ K_{\sigma\sigma 21}^{k\tau s} & K_{\sigma\sigma 22}^{k\tau s} & K_{\sigma\sigma 23}^{k\tau s} \\ K_{\sigma\sigma 31}^{k\tau s} & K_{\sigma\sigma 32}^{k\tau s} & K_{\sigma\sigma 33}^{k\tau s} \end{bmatrix} = \left[\begin{array}{c|c|c} \frac{C_{44}^k}{C_{45}^{k^2} - C_{44}^k C_{55}^k} J_{\alpha\beta}^{k\tau s} & \frac{C_{45}^k}{-C_{45}^{k^2} + C_{44}^k C_{55}^k} J_{\alpha\beta}^{k\tau s} & 0 \\ \frac{C_{45}^k}{-C_{45}^{k^2} + C_{44}^k C_{55}^k} J_{\alpha\beta}^{k\tau s} & \frac{C_{55}^k}{C_{45}^{k^2} - C_{44}^k C_{55}^k} J_{\alpha\beta}^{k\tau s} & 0 \\ 0 & 0 & -\frac{1}{C_{33}^k} J_{\alpha\beta}^{k\tau s} \end{array} \right] \quad (36)$$

The natural boundary conditions can be applied by computing firstly the matrix

$$\Pi_{uu}^{k\tau s} = \begin{bmatrix} \Pi_{uu11}^{k\tau s} & \Pi_{uu12}^{k\tau s} & \Pi_{uu13}^{k\tau s} \\ \Pi_{uu21}^{k\tau s} & \Pi_{uu22}^{k\tau s} & \Pi_{uu23}^{k\tau s} \\ \Pi_{uu31}^{k\tau s} & \Pi_{uu32}^{k\tau s} & \Pi_{uu33}^{k\tau s} \end{bmatrix} \quad (37)$$

$$\begin{aligned} \Pi_{uu11}^{k\tau s} = & n_\alpha \partial_\alpha^s C_{11}^k J_{\beta/\alpha}^{k\tau s} + n_\alpha \partial_\beta^s C_{16}^k J^{k\tau s} + n_\beta \partial_\alpha^s C_{16}^k J^{k\tau s} - n_\alpha \partial_\alpha^s \frac{C_{13}^{k^2}}{C_{33}^k} J_{\beta/\alpha}^{k\tau s} - \\ & n_\alpha \partial_\beta^s \frac{C_{13}^k C_{36}^k}{C_{33}^k} J^{k\tau s} - n_\beta \partial_\alpha^s \frac{C_{13}^k C_{36}^k}{C_{33}^k} J^{k\tau s} - n_\beta \partial_\beta^s \frac{C_{36}^{k^2}}{C_{33}^k} J_{\alpha/\beta}^{k\tau s} + n_\beta \partial_\beta^s C_{66}^k J_{\alpha/\beta}^{k\tau s} \end{aligned} \quad (38)$$

$$\begin{aligned} \Pi_{uu12}^{k\tau s} = & n_\alpha \partial_\beta^s C_{12}^k J^{k\tau s} + n_\alpha \partial_\alpha^s C_{16}^k J_{\beta/\alpha}^{k\tau s} + n_\beta \partial_\beta^s C_{26}^k J_{\alpha/\beta}^{k\tau s} - n_\alpha \partial_\beta^s \frac{C_{13}^k C_{23}^k}{C_{33}^k} J^{k\tau s} - \\ & n_\alpha \partial_\alpha^s \frac{C_{13}^k C_{36}^k}{C_{33}^k} J_{\beta/\alpha}^{k\tau s} - n_\beta \partial_\beta^s \frac{C_{23}^k C_{36}^k}{C_{33}^k} J_{\alpha/\beta}^{k\tau s} - n_\beta \partial_\alpha^s \frac{C_{36}^{k^2}}{C_{33}^k} J^{k\tau s} + n_\beta \partial_\alpha^s C_{66}^k J^{k\tau s} \end{aligned} \quad (39)$$

$$\begin{aligned} \Pi_{uu13}^{k\tau s} = & \frac{1}{R_\alpha^k} n_\beta C_{16}^k J^{k\tau s} + \frac{1}{R_\beta^k} n_\beta C_{26}^k J_{\alpha/\beta}^{k\tau s} - \frac{1}{R_\alpha^k} n_\beta \frac{C_{13}^k C_{36}^k}{C_{33}^k} J^{k\tau s} - \frac{1}{R_\beta^k} n_\beta \frac{C_{23}^k C_{36}^k}{C_{33}^k} J_{\alpha/\beta}^{k\tau s} + \\ & \frac{1}{R_\alpha^k} n_\alpha C_{11}^k J_{\beta/\alpha}^{k\tau s} + \frac{1}{R_\beta^k} n_\alpha C_{12}^k J^{k\tau s} - \frac{1}{R_\alpha^k} n_\alpha \frac{C_{13}^{k^2}}{C_{33}^k} J_{\beta/\alpha}^{k\tau s} - \frac{1}{R_\beta^k} n_\alpha \frac{C_{13}^k C_{23}^k}{C_{33}^k} J^{k\tau s} \end{aligned} \quad (40)$$

$$\begin{aligned} \Pi_{uu21}^{k\tau s} = & n_\beta \partial_\alpha^s C_{12}^k J^{k\tau s} + n_\alpha \partial_\alpha^s C_{16}^k J_{\beta/\alpha}^{k\tau s} + n_\beta \partial_\beta^s C_{26}^k J_{\alpha/\beta}^{k\tau s} - n_\beta \partial_\alpha^s \frac{C_{13}^k C_{23}^k}{C_{33}^k} J^{k\tau s} - \\ & n_\alpha \partial_\alpha^s \frac{C_{13}^k C_{36}^k}{C_{33}^k} J_{\beta/\alpha}^{k\tau s} - n_\beta \partial_\beta^s \frac{C_{23}^k C_{36}^k}{C_{33}^k} J_{\alpha/\beta}^{k\tau s} - n_\alpha \partial_\beta^s \frac{C_{36}^{k^2}}{C_{33}^k} J^{k\tau s} + n_\alpha \partial_\beta^s C_{66}^k J^{k\tau s} \end{aligned} \quad (41)$$

$$\begin{aligned}\Pi_{uu_{22}}^{k\tau s} = & n_\beta \partial_\beta^s C_{22}^k J_{\alpha/\beta}^{k\tau s} + n_\alpha \partial_\beta^s C_{26}^k J^{k\tau s} + n_\beta \partial_\alpha^s C_{26}^k J^{k\tau s} - n_\beta \partial_\beta^s \frac{C_{23}^{k^2}}{C_{33}^k} J_{\alpha/\beta}^{k\tau s} - \\ & n_\alpha \partial_\beta^s \frac{C_{23}^k C_{36}^k}{C_{33}^k} J^{k\tau s} - n_\beta \partial_\alpha^s \frac{C_{23}^k C_{36}^k}{C_{33}^k} J^{k\tau s} - n_\alpha \partial_\alpha^s \frac{C_{36}^{k^2}}{C_{33}^k} J_{\beta/\alpha}^{k\tau s} + n_\alpha \partial_\alpha^s C_{66}^k J_{\beta/\alpha}^{k\tau s}\end{aligned}\quad (42)$$

$$\begin{aligned}\Pi_{uu_{23}}^{k\tau s} = & \frac{1}{R_\alpha^k} n_\beta C_{12}^k J^{k\tau s} + \frac{1}{R_\beta^k} n_\beta C_{22}^k J_{\alpha/\beta}^{k\tau s} - \frac{1}{R_\alpha^k} n_\beta \frac{C_{13}^k C_{23}^k}{C_{33}^k} J^{k\tau s} - \frac{1}{R_\beta^k} n_\beta \frac{C_{23}^{k^2}}{C_{33}^k} J_{\alpha/\beta}^{k\tau s} + \\ & \frac{1}{R_\alpha^k} n_\alpha C_{16}^k J_{\beta/\alpha}^{k\tau s} + \frac{1}{R_\beta^k} n_\alpha C_{26}^k J^{k\tau s} - \frac{1}{R_\alpha^k} n_\alpha \frac{C_{13}^k C_{36}^k}{C_{33}^k} J_{\beta/\alpha}^{k\tau s} - \frac{1}{R_\beta^k} n_\alpha \frac{C_{23}^k C_{36}^k}{C_{33}^k} J^{k\tau s}\end{aligned}\quad (43)$$

$$\Pi_{uu_{31}}^{k\tau s} = 0 \quad (44)$$

$$\Pi_{uu_{32}}^{k\tau s} = 0 \quad (45)$$

$$\Pi_{uu_{33}}^{k\tau s} = 0 \quad (46)$$

In a similar way, we can impose boundary conditions in terms of the transverse stresses as

$$\begin{aligned}\Pi_{\sigma_{11}}^{k\tau s} = 0; \quad \Pi_{\sigma_{12}}^{k\tau s} = 0; \quad \Pi_{\sigma_{13}}^{k\tau s} = & n_\alpha \frac{C_{13}^k}{C_{33}^k} J_\beta^{k\tau s} + n_\beta \frac{C_{36}^k}{C_{33}^k} J_\alpha^{k\tau s} \\ \Pi_{\sigma_{21}}^{k\tau s} = 0; \quad \Pi_{\sigma_{22}}^{k\tau s} = 0; \quad \Pi_{\sigma_{23}}^{k\tau s} = & n_\beta \frac{C_{23}^k}{C_{33}^k} J_\alpha^{k\tau s} + n_\alpha \frac{C_{36}^k}{C_{33}^k} J_\beta^{k\tau s} \\ \Pi_{\sigma_{31}}^{k\tau s} = n_\alpha J_\beta^{k\tau s}; \quad \Pi_{\sigma_{32}}^{k\tau s} = n_\beta J_\alpha^{k\tau s}; \quad \Pi_{\sigma_{33}}^{k\tau s} = & 0\end{aligned}\quad (47)$$

The dynamic problem is expressed as:

$$\begin{aligned}& \sum_{k=1}^{N_l} \int_{\Omega_k} \int_{A_k} \left\{ \delta \epsilon_{pG}^{kT} \sigma_{pC}^k + \delta \epsilon_{nG}^{kT} \sigma_{nM}^k + \delta \sigma_{nM}^{kT} (\epsilon_{nG}^k - \epsilon_{nC}^k) \right\} H_\alpha H_\beta d\Omega_k dz = \\ & \sum_{k=1}^{N_l} \int_{\Omega_k} \int_{A_k} \rho^k \delta \mathbf{u}^{kT} \ddot{\mathbf{u}}^k H_\alpha H_\beta d\Omega_k dz + \sum_{k=1}^{N_l} \delta L_e^k\end{aligned}\quad (48)$$

where ρ^k is the mass density of the k -th layer and double dots denote acceleration.

By substituting the geometrical relations, the constitutive equations and the

Unified Formulation, we obtain the following governing equations:

$$\delta \mathbf{u}_s^{kT} : \quad \mathbf{K}_{uu}^{*k\tau s} \mathbf{u}_\tau^k = \mathbf{M}^{k\tau s} \ddot{\mathbf{u}}_\tau^k + \mathbf{P}_{u\tau}^k \quad (49)$$

In the case of free vibrations, the fundamental nucleus of the external work is $\mathbf{P}_{u\tau}^k = 0$ and one has:

$$\delta \mathbf{u}_s^{kT} : \quad \mathbf{K}_{uu}^{*k\tau s} \mathbf{u}_\tau^k = \mathbf{M}^{k\tau s} \ddot{\mathbf{u}}_\tau^k \quad (50)$$

where $\mathbf{K}_{uu}^{*k\tau s} = \mathbf{K}_{uu}^{k\tau s} - \mathbf{K}_{u\sigma}^{k\tau s} [\mathbf{K}_{\sigma\sigma}^{k\tau s}]^{-1} \mathbf{K}_{\sigma u}^{k\tau s}$ and it is obtained after a static condensation procedure.

$\mathbf{M}^{k\tau s}$ is the fundamental nucleus for the inertial term. The explicit form of that is:

$$M_{11}^{k\tau s} = \rho^k F_\tau F_s; \quad M_{12}^{k\tau s} = 0; \quad M_{13}^{k\tau s} = 0 \quad (51)$$

$$M_{21}^{k\tau s} = 0; \quad M_{22}^{k\tau s} = \rho^k F_\tau F_s; \quad M_{23}^{k\tau s} = 0 \quad (52)$$

$$M_{31}^{k\tau s} = 0; \quad M_{32}^{k\tau s} = 0; \quad M_{33}^{k\tau s} = \rho^k F_\tau F_s \quad (53)$$

At this point, we would like to note that the same radial basis functions are used for the interpolation of all the unknowns, displacements and stresses alike.

5 The radial basis function method

5.1 The static problem

Radial basis functions (RBF) approximations are mesh-free numerical schemes that can exploit accurate representations of the boundary, are easy to implement and can be spectrally accurate. In this section the formulation of a global unsymmetrical collocation RBF-based method to compute elliptic operators is presented.

Consider a linear elliptic partial differential operator L and a bounded region Ω in \mathbb{R}^n with some boundary $\partial\Omega$. In the static problems we seek the computation of displacements (\mathbf{u}) from the global system of equations

$$\mathcal{L}\mathbf{u} = \mathbf{f} \text{ in } \Omega \quad (54)$$

$$\mathcal{L}_B \mathbf{u} = \mathbf{g} \text{ on } \partial\Omega \quad (55)$$

where \mathcal{L} , \mathcal{L}_B are linear operators in the domain and on the boundary, respectively. The right-hand side of (54) and (55) represent the external forces applied on the plate or shell and the boundary conditions applied along the perimeter of the plate or shell, respectively. The PDE problem defined in (54) and (55) will be replaced by a finite problem, defined by an algebraic system of equations, after the radial basis expansions.

5.2 The eigenproblem

The eigenproblem looks for eigenvalues (λ) and eigenvectors (\mathbf{u}) that satisfy

$$\mathcal{L}\mathbf{u} + \lambda\mathbf{u} = 0 \text{ in } \Omega \quad (56)$$

$$\mathcal{L}_B\mathbf{u} = 0 \text{ on } \partial\Omega \quad (57)$$

As in the static problem, the eigenproblem defined in (56) and (57) is replaced by a finite-dimensional eigenvalue problem, based on RBF approximations.

5.3 Radial basis functions approximations

The radial basis function (ϕ) approximation of a function (\mathbf{u}) is given by

$$\tilde{\mathbf{u}}(\mathbf{x}) = \sum_{i=1}^N \alpha_i \phi(\|\mathbf{x} - \mathbf{y}_i\|_2), \mathbf{x} \in \mathbb{R}^n \quad (58)$$

where $\mathbf{y}_i, i = 1, \dots, N$ is a finite set of distinct points (centers) in \mathbb{R}^n . Note that, from this point on, we use x, y, z to avoid confusion with other symbols. Actually, one has to consider that we mean α, β, z and all the variables expressed in the curvilinear reference system.

The most common RBFs are

$$\begin{aligned} \text{Cubic:} \quad & \phi(r) = r^3 \\ \text{Thin plate splines:} \quad & \phi(r) = r^2 \log(r) \\ \text{Wendland functions:} \quad & \phi(r) = (1 - r)_+^m p(r) \\ \text{Gaussian:} \quad & \phi(r) = e^{-(cr)^2} \\ \text{Multiquadrics:} \quad & \phi(r) = \sqrt{c^2 + r^2} \\ \text{Inverse Multiquadrics:} \quad & \phi(r) = (c^2 + r^2)^{-1/2} \end{aligned}$$

where the Euclidian distance r is real and non-negative and c is a positive shape parameter.

Hardy [53] introduced multiquadrics in the analysis of scattered geographical data. In the 1990's Kansa [24] used multiquadrics for the solution of partial differential equations. Considering N distinct interpolations, and knowing $u(x_j), j = 1, 2, \dots, N$, we find α_i by the solution of a $N \times N$ linear system

$$\mathbf{A}\boldsymbol{\alpha} = \mathbf{u} \quad (59)$$

where $\mathbf{A} = [\phi(\|x - y_i\|_2)]_{N \times N}$, $\boldsymbol{\alpha} = [\alpha_1, \alpha_2, \dots, \alpha_N]^T$ and $\mathbf{u} = [u(x_1), u(x_2), \dots, u(x_N)]^T$.

5.4 Solution of the static problem

The solution of a static problem by radial basis functions considers N_I nodes in the domain and N_B nodes on the boundary, with a total number of nodes $N = N_I + N_B$. We denote the sampling points by $x_i \in \Omega, i = 1, \dots, N_I$ and $x_i \in \partial\Omega, i = N_I + 1, \dots, N$. At the points in the domain we solve the following system of equations

$$\sum_{i=1}^N \alpha_i \mathcal{L}\phi(\|x - y_i\|_2) = \mathbf{f}(x_j), j = 1, 2, \dots, N_I \quad (60)$$

or

$$\mathcal{L}^I \boldsymbol{\alpha} = \mathbf{F} \quad (61)$$

where

$$\mathcal{L}^I = [\mathcal{L}\phi(\|x - y_i\|_2)]_{N_I \times N} \quad (62)$$

At the points on the boundary, we impose boundary conditions as

$$\sum_{i=1}^N \alpha_i \mathcal{L}_B \phi(\|x - y_i\|_2) = \mathbf{g}(x_j), j = N_I + 1, \dots, N \quad (63)$$

or

$$\mathbf{B}\boldsymbol{\alpha} = \mathbf{G} \quad (64)$$

where

$$\mathbf{B} = \mathcal{L}_B \phi(\|x_{N_I+1} - y_j\|_2)_{N_B \times N}$$

Therefore, we can write a finite-dimensional static problem as

$$\begin{bmatrix} \mathcal{L}^I \\ \mathbf{B} \end{bmatrix} \boldsymbol{\alpha} = \begin{bmatrix} \mathbf{F} \\ \mathbf{G} \end{bmatrix} \quad (65)$$

By inverting the system (65), we obtain the vector $\boldsymbol{\alpha}$. We then obtain the solution \mathbf{u} using the interpolation equation (58).

5.5 Solution of the eigenproblem

We consider N_I nodes in the interior of the domain and N_B nodes on the boundary, with $N = N_I + N_B$. We denote interpolation points by $x_i \in \Omega, i = 1, \dots, N_I$ and $x_i \in \partial\Omega, i = N_I + 1, \dots, N$. At the points in the domain, we define the eigenproblem as

$$\sum_{i=1}^N \alpha_i \mathcal{L}\phi(\|x - y_i\|_2) = \lambda \tilde{\mathbf{u}}(x_j), j = 1, 2, \dots, N_I \quad (66)$$

or

$$\mathcal{L}^I \boldsymbol{\alpha} = \lambda \tilde{\mathbf{u}}^I \quad (67)$$

where

$$\mathcal{L}^I = [\mathcal{L}\phi(\|x - y_i\|_2)]_{N_I \times N} \quad (68)$$

At the points on the boundary, we enforce the boundary conditions as

$$\sum_{i=1}^N \alpha_i \mathcal{L}_B \phi(\|x - y_i\|_2) = 0, j = N_I + 1, \dots, N \quad (69)$$

or

$$\mathbf{B} \boldsymbol{\alpha} = 0 \quad (70)$$

Equations (67) and (70) can now be solved as a generalized eigenvalue problem

$$\begin{bmatrix} \mathcal{L}^I \\ \mathbf{B} \end{bmatrix} \boldsymbol{\alpha} = \lambda \begin{bmatrix} \mathbf{A}^I \\ \mathbf{0} \end{bmatrix} \boldsymbol{\alpha} \quad (71)$$

where

$$\mathbf{A}^I = \phi(\|x_{N_I} - y_j\|_2)_{N_I \times N}$$

5.6 Discretization of the equations of motion and boundary conditions

The radial basis collocation method follows a simple implementation procedure. Taking equation (13), we compute

$$\boldsymbol{\alpha} = \begin{bmatrix} L^I \\ \mathbf{B} \end{bmatrix}^{-1} \begin{bmatrix} \mathbf{F} \\ \mathbf{G} \end{bmatrix} \quad (72)$$

This $\boldsymbol{\alpha}$ vector is then used to obtain solution $\tilde{\mathbf{u}}$, by using (7). If derivatives of $\tilde{\mathbf{u}}$ are needed, such derivatives are computed as

$$\frac{\partial \tilde{\mathbf{u}}}{\partial x} = \sum_{j=1}^N \alpha_j \frac{\partial \phi_j}{\partial x} \quad (73)$$

$$\frac{\partial^2 \tilde{\mathbf{u}}}{\partial x^2} = \sum_{j=1}^N \alpha_j \frac{\partial^2 \phi_j}{\partial x^2}, \text{ etc} \quad (74)$$

In the present collocation approach, we need to impose essential and natural boundary conditions. Consider, for example, the condition $w = 0$, on a simply supported or clamped edge. We enforce the conditions by interpolating as

$$w = 0 \rightarrow \sum_{j=1}^N \alpha_j^W \phi_j = 0 \quad (75)$$

Other boundary conditions are interpolated in a similar way.

5.7 Free vibrations problems

For free vibration problems we set the external force to zero, and assume harmonic solution in terms of displacements $u_1, u_2, \dots, v_1, v_2, \dots$, as

$$u_1 = U_1(w, y)e^{i\omega t}; \quad u_2 = U_2(w, y)e^{i\omega t}; \quad u_3 = U_3(w, y)e^{i\omega t}; \quad u_4 = U_4(w, y)e^{i\omega t} \quad (76)$$

$$v_1 = V_1(w, y)e^{i\omega t}; \quad v_2 = V_2(w, y)e^{i\omega t}; \quad v_3 = V_3(w, y)e^{i\omega t}; \quad v_4 = V_4(w, y)e^{i\omega t} \quad (77)$$

$$w_1 = W_1(w, y)e^{i\omega t}; \quad w_2 = W_2(w, y)e^{i\omega t}; \quad w_3 = W_3(w, y)e^{i\omega t}; \quad w_4 = W_4(w, y)e^{i\omega t} \quad (78)$$

where ω is the frequency of natural vibration. Substituting the harmonic expansion into equations (71) in terms of the displacements and transverse

stresses, we may obtain the natural frequencies and vibration modes for the plate or shell problem, by solving the eigenproblem

$$[\mathcal{L} - \omega^2 \mathcal{G}] \mathbf{X} = \mathbf{0} \quad (79)$$

where \mathcal{L} collects all stiffness terms and \mathcal{G} collects all terms related to the inertial terms. In (79) \mathbf{X} are the modes of vibration associated with the natural frequencies defined as ω .

6 Computation of stresses

Taking into account the large number of degrees of freedom per node, the solution of the static problem is obtained after a static condensation procedure as follows. Consider the global system of equations (after imposing boundary conditions):

$$\begin{bmatrix} \mathbf{K}_{uu} & \mathbf{K}_{u\sigma} \\ \mathbf{K}_{\sigma u} & \mathbf{K}_{\sigma\sigma} \end{bmatrix} \begin{bmatrix} \mathbf{u} \\ \boldsymbol{\sigma} \end{bmatrix} = \begin{bmatrix} \mathbf{f} \\ \mathbf{0} \end{bmatrix} \quad (80)$$

The problem is reduced to

$$\mathbf{K}^*_{uu} \mathbf{u} = \mathbf{f} \quad (81)$$

where $\mathbf{K}^*_{uu} = \mathbf{K}_{uu} - \mathbf{K}_{u\sigma}[\mathbf{K}_{\sigma\sigma}]^{-1}\mathbf{K}_{\sigma u}$. After computation of the solution, transverse stresses are readily computed at each interface by

$$\boldsymbol{\sigma} = [\mathbf{K}_{\sigma\sigma}]^{-1} (-\mathbf{K}_{\sigma u} \mathbf{u}) \quad (82)$$

7 Numerical examples

All numerical examples consider a Chebyshev grid and a Wendland function, defined as

$$\phi(r) = (1 - c r)_+^8 \left(32(c r)^3 + 25(c r)^2 + 8c r + 1 \right) \quad (83)$$

where the shape parameter (c) was obtained by an optimization procedure, as detailed in Ferreira and Fasshauer [54].

7.1 Spherical shell in bending

A laminated composite spherical shell is here considered, of side a and thickness h , composed of equal thickness layers oriented at $[0^\circ/90^\circ/0^\circ]$ and $[0^\circ/90^\circ/90^\circ/0^\circ]$. The shell is subjected to a sinusoidal vertical pressure of the form

$$p_z = P \sin\left(\frac{\pi x}{a}\right) \sin\left(\frac{\pi y}{a}\right)$$

with the origin of the coordinate system located at the lower left corner on the midplane and P the maximum load (at center of shell).

The orthotropic material properties for each layer are given by

$$E_1 = 25.0E_2 \quad G_{12} = G_{13} = 0.5E_2 \quad G_{23} = 0.2E_2 \quad \nu_{12} = 0.25$$

The transverse displacements are presented in normalized form as $\bar{w} = \frac{10^3 w_{(a/2, a/2, 0)} h^3 E_2}{Pa^4}$.

The shell is simply-supported on all edges.

In table 1, an assessment of the present model is presented for the plate case ($R \rightarrow \infty$). We compare the deflections obtained with the RBF method with the LW analytical solution given in [45] and the results obtained with two different shell finite elements: MITC4 and MITC9. These elements are based on CUF and they are described in details in [56] and [57], respectively. Various thickness ratios and laminations are considered. In all the cases, the table shows that the present method is in good agreement with the FEM solution.

In table 2 we compare the static deflections for the present shell model with results of Reddy shell formulation using first-order and third-order shear-deformation theories [55] and the LW analytical solution given in [45]. We consider nodal grids with 13×13 , 17×17 , and 21×21 points. We consider various values of R/a and two values of a/h (10 and 100). Results are in good agreement for various a/h ratios with the higher-order results of Reddy and the LW analytical solution.

In figure 3 it is illustrated the evolution of the transverse shear stresses τ_{xz} , for $a/h = 10$, laminate $[0^\circ/90^\circ/0^\circ]$. As can be seen, the formulation does not produce zero top and bottom shear stresses, for two reasons. First, the formulation is not based on C^1 definition of transverse displacement, and second the load is not applied at the middle surface, but at the top surface. As can also be seen, because of the mixed formulation, and consideration of transverse stress variables at each interface, the transverse stresses are continuous at the laminate interfaces.

	Method	$a/h = 10$	$a/h = 100$
[0°/90°/0°]	LW [45]	7.4095	4.3400
	present (13 × 13)	7.3985	4.3065
	present (17 × 17)	7.3980	4.3063
	present (21 × 21)	7.3979	4.3062
	MITC4 (13 × 13)	7.2955	4.2573
	MITC4 (17 × 17)	7.3427	4.2915
	MITC4 (21 × 21)	7.3657	4.3082
	MITC9 (5 × 5)	7.4067	4.3375
	MITC9 (9 × 9)	7.4092	4.3397
	MITC9 (13 × 13)	7.4095	4.3399
[0°/90°/90°/0°]	LW [45]	7.3148	4.3420
	present (13 × 13)	7.3551	4.3058
	present (17 × 17)	7.3547	4.3056
	present (21 × 21)	7.3545	4.3054
	MITC4 (13 × 13)	7.2011	4.2593
	MITC4 (17 × 17)	7.2482	4.2935
	MITC4 (21 × 21)	7.2711	4.3102
	MITC9 (5 × 5)	7.3120	4.3396
	MITC9 (9 × 9)	7.3145	4.3418
	MITC9 (13 × 13)	7.3147	4.3420

Table 1

Non-dimensional central deflection, $\bar{w} = w \frac{10^3 E_2 h^3}{P_0 a^4}$ for different cross-ply laminated plates.

In figure 4 it is illustrated the evolution of the normal stresses σ_{xx} , for $a/h = 10$, laminate [0°/90°/0°]. In both figures, a Chebyshev 17×17 grid was considered.

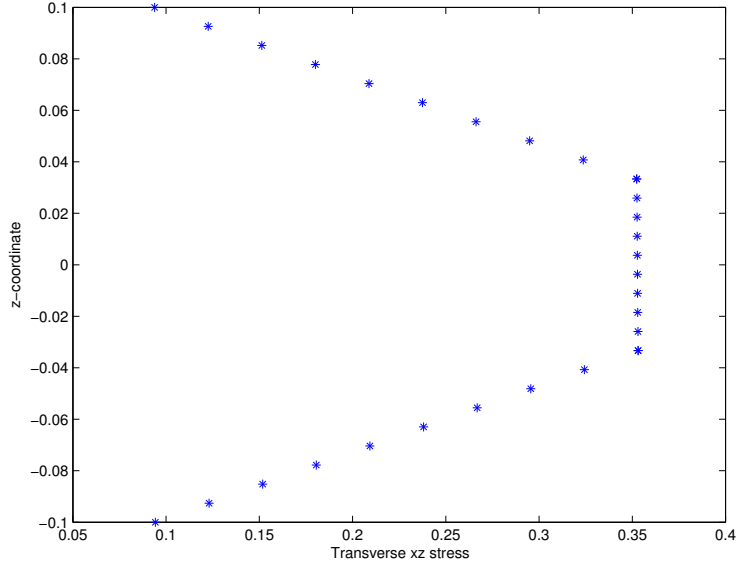


Fig. 3. Evolution of the transverse shear stresses τ_{xz} , for $a/h = 10$, laminate $[0^\circ/90^\circ/0^\circ]$.

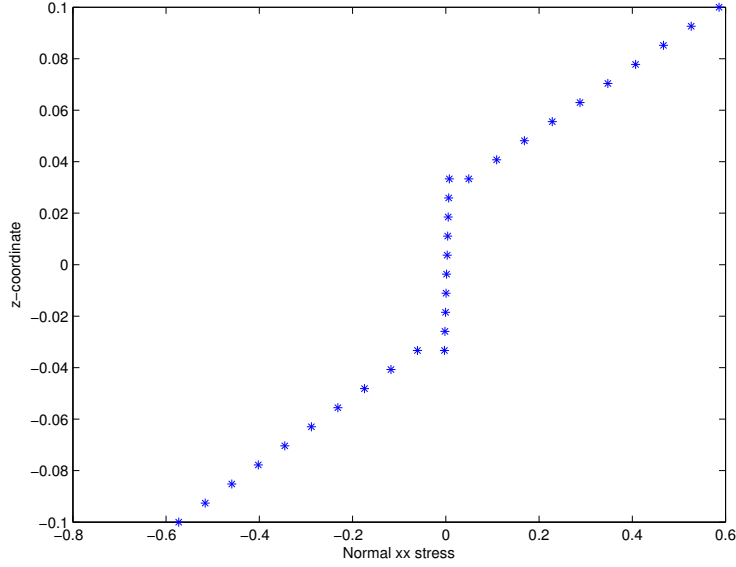


Fig. 4. Evolution of the normal stresses σ_{xx} , for $a/h = 10$, laminate $[0^\circ/90^\circ/0^\circ]$.

7.2 Free vibration of spherical and cylindrical laminated shells

We consider nodal grids with 13×13 , 17×17 , and 21×21 points. In tables 3 and 4 we compare the nondimensionalized natural frequencies from the present layerwise theory for various cross-ply spherical shells, with analytical solutions

by Reddy and Liu [55] who considered both the first-order (FSDT) and the third-order (HSDT) theories. The first-order theory overpredicts the fundamental natural frequencies of symmetric thick shells and symmetric shallow thin shells. The present radial basis function method is compared with analytical results by Reddy [55] and shows excellent agreement.

Table 5 contain nondimensionalized natural frequencies obtained using the the present layerwise theory for cross-ply cylindrical shells with lamination schemes $[0/90/0]$, $[0/90/90/0]$. Present results are compared with analytical solutions by Reddy and Liu [55] who considered both the first-order (FSDT) and the third-order (HSDT) theories. The present radial basis function method is compared with analytical results by Reddy [55] and shows excellent agreement.

8 Concluding remarks

In this paper a Reissner Mixed Variational Theorem was implemented for the first time for laminated orthotropic elastic shells through a RBF discretization of equations of motion and boundary conditions. The radial basis function method with a Wendland function was presented for the solution of shell bending and free vibration problems. Results for static deformations and natural frequencies were obtained and compared with other sources. This meshless approach demonstrated that is very successful in the static deformations and free vibration analysis of laminated composite shells. Advantages of radial basis functions are absence of mesh, ease of discretization of boundary conditions and equations of equilibrium or motion and very easy coding. We show that the static displacements and stresses and the natural frequencies obtained from present method are in excellent agreement with analytical or reference solutions.

9 Acknowledgements

A. J. M. Ferreira acknowledges the kind support of Fundação para a Ciência e Tecnologia, to project PTDC/EMC-PRO/2044/201.

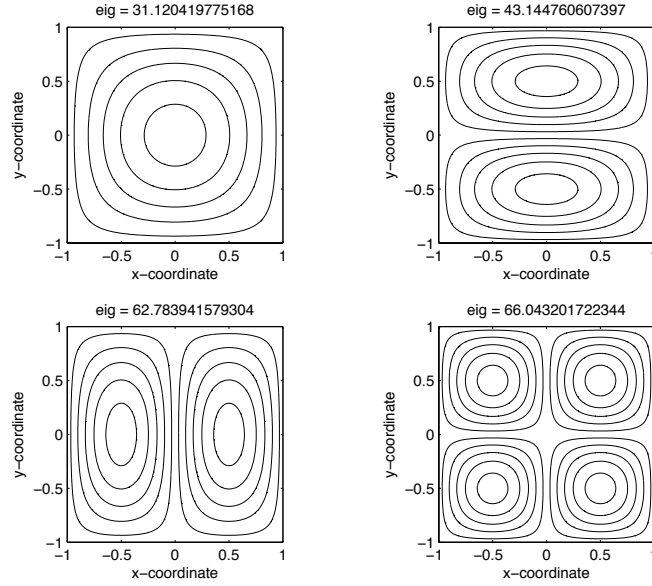


Fig. 5. First 4 vibrational modes of cross-ply laminated spherical shells, $\bar{\omega} = \omega \frac{a^2}{h} \sqrt{\rho/E_2}$, laminate $([0^\circ/90^\circ/90^\circ/0^\circ])$ grid 13×13 points, $a/h = 100$, $R/a = 10$

References

- [1] E. I. Grigolyuk and G. M. Kulikov. General direction of the development of the theory of shells. *Mekhanika Kompozitnykh Materialov*, 2:287–298, 1988.
- [2] R. K. Kapania and S. Raciti. Recent advances in analysis of laminated beams and plates. *American Institute of Aeronautics and Astronautics Journal*, 27:923–946, 1989.
- [3] R. K. Kapania. A review on the analysis of laminated shells. *Journal of Pressure Vessel Technology*, 111:88–96, 1989.
- [4] A. K. Noor and W. S. Burton. Assessment of shear deformation theories for multilayered composite plates. *Applied Mechanics Review*, 41:1–18, 1989.
- [5] A. K. Noor and W. S. Burton. Assessment of computational models for multilayered composite shells. *Applied Mechanics Review*, 43:67–97, 1990.
- [6] A. K. Noor, W. S. Burton and C. W. Bert. Computational model for sandwich panels and shells. *Applied Mechanics Review*, 49:155–199, 1996.
- [7] K. P. Soldatos and T. Timarci. A unified formulation of laminated composites, shear deformable, five-degrees-of-freedom cylindrical shell theories. *Composite Structures*, 25:165–171, 1993.
- [8] I. F. Pinto Correia, P. G. Martins, C. M. Mota Soares, C. A. Mota Soares, and J. Herskovits. Modelling and optimization of laminated adaptive shells of revolution. *Composite Structures*, 75:49–59, 2006.

- [9] A. M. A. Neves, A. J. M. Ferreira, E. Carrera, M. Cinefra, C. M. C. Roque, R. M. N. Jorge, and C. M. M. Soares. Free vibration analysis of functionally graded shells by a higher-order shear deformation theory and radial basis functions collocation, accounting for through-the-thickness deformations. *European Journal of Mechanics - A/Solids*, 37:24–34, 2013.
- [10] J. N. Reddy. *Mechanics of Laminated Composite Plates, Theory and Analysis*. Boca Raton: CRC Press, 1997.
- [11] T. Hsu and J. T. Wang. A theory of laminated cylindrical shells consisting of layers of orthotropic laminae. *American Institute of Aeronautics and Astronautics Journal*, 8:2141–2146, 1970.
- [12] Y. K. Cheung and C. I. Wu. Free vibrations of thick, layered cylinders having finite length with various boundary conditions. *Journal of Sound and Vibration*, 24:189–200, 1972.
- [13] S. Srinivas. A refined analysis of composite laminates. *Journal of Sound and Vibration*, 30:495–550, 1973.
- [14] C. T. Sun and J. M. Whitney. On the theories for the dynamic response of laminated plates. *American Institute of Aeronautics and Astronautics Journal*, 11:372–398, 1973.
- [15] E. J. Barbero, J. N. Reddy and J. L. Teply. General two-dimensional theory of laminated cylindrical shells. *American Institute of Aeronautics and Astronautics Journal*, 28:544–553, 1990.
- [16] K. N. Cho, C. W. Bert and A. G. Striz. Free vibrations of laminated rectangular plates analyzed by higher order individual-layer theory. *Journal of Sound and Vibration*, 145:429–442, 1991.
- [17] A. Nosier, R. K. Kapania and J. N. Reddy. Free vibration analysis of laminated plates using a layer-wise theory. *American Institute of Aeronautics and Astronautics Journal*, 31:2335–2346, 1993.
- [18] P. Gaudenzi, R. Barboni and A. Mannini. A finite element evaluation of single-layer and multi-layer theories for the analysis of laminated plates. *Composite Structures*, 30:427–440, 1995.
- [19] E. Carrera. Evaluation of layer-wise mixed theories for laminated plates analysis. *American Institute of Aeronautics and Astronautics Journal*, 36:830–839, 1998.
- [20] E. Carrera. Layer-wise mixed models for accurate vibration analysis of multilayered plates. *Journal of Applied Mechanics*, 65:820–828, 1998.
- [21] S. T. Dennis and A. N. Palazotto. Transverse shear deformation in orthotropic cylindrical pressure vessels using a higher-order shear theory. *AIAA Journal*, 27(10):1441–1447, 1989.
- [22] J. Merk. Hierarchische, Kontinuumbasiert Shalenelemente höhere Ordnung *Ph.D Dissertation*, Inst. for Statics and Dynamics, Universität Stuttgart, Stuttgart, Germany, 1995.

- [23] S. Di and E. Ramm. Hybrid stress formulation for higher-order theory of laminated shell analysis. *Computer Method in Applied Mechanics and Engineering*, 109:359–356, 1993.
- [24] E. J. Kansa. Multiquadrics- a scattered data approximation scheme with applications to computational fluid dynamics. i: Surface approximations and partial derivative estimates. *Computers and Mathematics with Applications*, 19(8/9):127–145, 1990.
- [25] Y. C. Hon, M. W. Lu, W. M. Xue, and Y. M. Zhu. Multiquadric method for the numerical solution of byphasic mixture model. *Applied Mathematics and Computation*, 88:153–175, 1997.
- [26] Y. C. Hon, K. F. Cheung, X. Z. Mao, and E. J. Kansa. A multiquadric solution for the shallow water equation. *ASCE Journal of Hydraulic Engineering*, 125(5):524–533, 1999.
- [27] J. G. Wang, G. R. Liu, and P. Lin. Numerical analysis of biot’s consolidation process by radial point interpolation method. *International Journal of Solids and Structures*, 39(6):1557–1573, 2002.
- [28] G. R. Liu and Y. T. Gu. A local radial point interpolation method (lrpim) for free vibration analyses of 2-d solids. *Journal of Sound and Vibration*, 246(1):29–46, 2001.
- [29] G. R. Liu and J. G. Wang. A point interpolation meshless method based on radial basis functions. *International Journal for Numerical Methods in Engineering*, 54:1623–1648, 2002.
- [30] J. G. Wang and G. R. Liu. On the optimal shape parameters of radial basis functions used for 2-d meshless methods. *Computer Methods in Applied Mechanics and Engineering*, 191:2611–2630, 2002.
- [31] X. L. Chen, G. R. Liu, and S. P. Lim. An element free galerkin method for the free vibration analysis of composite laminates of complicated shape. *Composite Structures*, 59:279–289, 2003.
- [32] K. Y. Dai, G. R. Liu, S. P. Lim, and X. L. Chen. An element free galerkin method for static and free vibration analysis of shear-deformable laminated composite plates. *Journal of Sound and Vibration*, 269:633–652, 2004.
- [33] G. R. Liu and X. L. Chen. Buckling of symmetrically laminated composite plates using the element-free galerkin method. *International Journal of Structural Stability and Dynamics*, 2:281–294, 2002.
- [34] K. M. Liew, X. L. Chen, and J. N. Reddy. Mesh-free radial basis function method for buckling analysis of non-uniformity loaded arbitrarily shaped shear deformable plates. *Computer Methods in Applied Mechanics and Engineering*, 193:205–225, 2004.
- [35] Y. Q. Huang and Q. S. Li. Bending and buckling analysis of antisymmetric laminates using the moving least square differential quadrature method. *Computer Methods in Applied Mechanics and Engineering*, 193:3471–3492, 2004.

- [36] L. Liu, G. R. Liu, and V. C. B. Tan. Element free method for static and free vibration analysis of spatial thin shell structures. *Computer Methods in Applied Mechanics and Engineering*, 191:5923–5942, 2002.
- [37] S. Xiang, K. M. Wang, Y. T. Ai, Y. D. Sha, and H. Shi. Analysis of isotropic, sandwich and laminated plates by a meshless method and various shear deformation theories. *Composite Structures*, 91(1):31–37, 2009.
- [38] S. Xiang, H. Shi, K. M. Wang, Y. T. Ai, and Y. D. Sha. Thin plate spline radial basis functions for vibration analysis of clamped laminated composite plates. *European Journal of Mechanics A/Solids*, 29:844–850, 2010.
- [39] Ferreira A. J. A. Roque, C. M. C. and R. M. N. Jorge. Analysis of composite and sandwich plate by trigonometric layer-wise deformation theory and radial basis function. *J. Sandwich Struct. Mater.*, 8:497–515, 2006.
- [40] A. J. M. Ferreira. A formulation of the multiquadric radial basis function method for the analysis of laminated composite plates. *Composite Structures*, 59:385–392, 2003.
- [41] A. J. M. Ferreira. Thick composite beam analysis using a global meshless approximation based on radial basis functions. *Mechanics of Advanced Materials and Structures*, 10:271–284, 2003.
- [42] A. J. M. Ferreira, C. M. C. Roque, and P. A. L. S. Martins. Analysis of composite plates using higher-order shear deformation theory and a finite point formulation based on the multiquadric radial basis function method. *Composites: Part B*, 34:627–636, 2003.
- [43] E. Carrera. Theories and finite elements for multilayered plates and shells: a unified compact formulation with numerical assessment and benchmarking. *Arch Comput Methods Eng*, 97:10–215, 2003.
- [44] E. Carrera. Multilayered shell theories accounting for layerwise mixed description, part 1: governing equations. *AIAA Journal*, 37(9):1107–1116, 1999.
- [45] E. Carrera. Multilayered shell theories accounting for layerwise mixed description, part 2: numerical evaluations. *AIAA Journal*, 37(9):1117–1124, 1999.
- [46] E. Carrera. A study of transverse normal stress effect on vibration of multilayered plates and shells. *Journal of Sound and Vibration*, 225(5):803–829, 1999.
- [47] E. Carrera. A Reissner’s mixed variational theorem applied to vibrational analysis of multilayered shell. *Journal of Applied Mechanics*, 66:63–78, 1998.
- [48] E. Carrera. Developments, ideas, and evaluations based upon reissner’s mixed variational theorem in the modelling of multilayered plates and shells. *Applied Mechanics Reviews*, 54:301–329, 2001.
- [49] E. Carrera. C^0 reissner-mindlin multilayered plate elements including zig-zag and interlaminar stress continuity. *International Journal of Numerical Methods in Engineering*, 39:1797–1820, 1996.

- [50] E. Carrera and B. Kroplin. Zig-zag and interlaminar equilibria effects in large deflection and post-buckling analysis of multilayered plates. *Mechanics of Composite Materials and Structures*, 4:69–94, 1997.
- [51] A. W. Leissa. *Vibration of Shells*. NASA SP-288, Washington, D.C. (USA), 1973.
- [52] I. S. Sokolnikoff. *Mathematical Theory of Elasticity*. McGraw-Hill, Book Company Inc., New York (USA), 1956.
- [53] R. L. Hardy. Multiquadric equations of topography and other irregular surfaces. *Geophysical Research*, 176:1905–1915, 1971.
- [54] A. J. M. Ferreira and G. E. Fasshauer. Computation of natural frequencies of shear deformable beams and plates by a rbf-pseudospectral method. *Computer Methods in Applied Mechanics and Engineering*, 196:134–146, 2006.
- [55] J. N. Reddy and C. F. Liu. A higher-order shear deformation theory of laminated elastic shells. *International Journal of Engineering Science*, 23:319–330, 1985.
- [56] M. Cinefra, E. Carrera and P. Nali. MITC technique extended to variable kinematic multilayered plate elements. *Composite Structures*, 92:1888–1895, 2010.
- [57] M. Cinefra, C. Chinosi and L. Della Croce. MITC9 shell elements based on refined theories for the analysis of isotropic cylindrical structures. *Mechanics of Advanced Materials and Structures*, 20:91–100, 2013.

			Method		R/a					
			a/h		5	10	20	50	100	10^9
$[0^\circ/90^\circ/0^\circ]$	10	present	(13×13)		7.0506	7.2603	7.3286	7.3496	7.3532	7.3551
	10	present	(17×17)		7.0505	7.2599	7.3281	7.3492	7.3528	7.3547
	10	present	(21×21)		7.0503	7.2598	7.3280	7.3490	7.3526	7.3545
	10	HSDT	[55]		6.7688	7.0325	7.1016	7.1212	7.1240	7.125
	10	FSDT	[55]		6.4253	6.6247	6.6756	6.6902	6.6923	6.6939
	10	LW	[45]		7.0834	7.3252	7.3883	7.4061	7.4087	7.4095
	100	present	(13×13)		1.0251	2.3920	3.5881	4.1702	4.2716	4.3058
	100	present	(17×17)		1.0255	2.3925	3.5882	4.1721	4.2714	4.3056
	100	present	(21×21)		1.0255	2.3925	3.5882	4.1721	4.2714	4.3056
	100	HSDT	[55]		1.0321	2.4099	3.617	4.2071	4.3074	4.3420
	100	FSDT	[55]		1.0337	2.4109	3.6150	4.2027	4.3026	4.3370
	100	LW	[45]		1.0340	2.4120	3.6172	4.2055	4.3055	4.3400
$[0^\circ/90^\circ/90^\circ/0^\circ]$	10	present	(13×13)		7.0088	7.2603	7.3286	7.3496	7.3532	7.3551
	10	present	(17×17)		7.0086	7.2599	7.3281	7.3492	7.3528	7.3547
	10	present	(21×21)		7.0085	7.2598	7.3280	7.3490	7.3526	7.3545
	10	HSDT	[55]		6.7865	7.0536	7.1237	7.1436	7.1464	7.1474
	10	FSDT	[55]		6.3623	6.5595	6.6099	6.6244	6.6264	6.6280
	10	LW	[45]		6.9953	7.2322	7.2940	7.3114	7.3139	7.3148
	100	present	(13×13)		1.0251	2.3920	3.5881	4.1722	4.2716	4.3058
	100	present	(17×17)		1.0255	2.3925	3.5882	4.1721	4.2714	4.3056
	100	present	(21×21)		1.0255	2.3925	3.5882	4.1721	4.2714	4.3056
	100	HSDT	[55]		1.0264	2.4024	3.6133	4.2071	4.3082	4.3430
	100	FSDT	[55]		1.0279	2.4030	3.6104	4.2015	4.3021	4.3368
	100	LW	[45]		1.0284	2.4048	3.6142	4.2065	4.3073	4.3420

Table 2

Non-dimensional central deflection, $\bar{w} = w \frac{10^3 E_2 h^3}{P_0 a^4}$ variation with various number of grid points per unit length, N for different R/a ratios, for $R_1 = R_2$

a/h	Method	R/a					
		5	10	20	50	100	10^9
10	present (13×13)	11.8127	11.6433	11.6003	11.5882	11.5865	11.5859
	present (17×17)	11.8123	11.6431	11.6001	11.5881	11.5863	11.5858
	present (21×21)	11.8123	11.6431	11.6001	11.5881	11.5863	11.5858
	HSDT [55]	12.040	11.840	11.790	11.780	11.780	11.780
100	present (13×13)	31.1204	20.4266	16.6892	15.4798	15.2992	15.2385
	present (17×17)	31.1128	20.4235	16.6881	15.4794	15.2988	15.2382
	present (21×21)	31.1117	20.4231	16.6879	15.4793	15.2988	15.2382
	HSDT [55]	31.100	20.380	16.630	15.420	15.230	15.170

Table 3

Nondimensionalized fundamental frequencies of cross-ply laminated spherical shells, $\bar{\omega} = \omega \frac{a^2}{h} \sqrt{\rho/E_2}$, laminate ($[0^\circ/90^\circ/90^\circ/0^\circ]$)

a/h	Method	R/a					
		5	10	20	50	100	10^9
10	present (13×13)	11.7720	11.6033	11.5605	11.5484	11.5467	11.5461
	present (17×17)	11.7717	11.6031	11.5603	11.5483	11.5465	11.5460
	present (21×21)	11.7716	11.6031	11.5603	11.5483	11.5465	11.5460
	HSDT[55]	12.060	11.860	11.810	11.790	11.790	11.790
100	present (13×13)	31.0370	20.3936	16.6782	15.4768	15.2974	15.2371
	present (17×17)	31.0294	20.3905	16.6770	15.4763	15.2970	15.2368
	present (21×21)	31.0283	20.3901	16.6769	15.4763	15.2970	15.2368
	HSDT[55]	31.0398	20.350	16.620	15.420	15.240	15.170

Table 4

Nondimensionalized fundamental frequencies of cross-ply laminated spherical shells, $\bar{\omega} = \omega \frac{a^2}{h} \sqrt{\rho/E_2}$, laminate ($[0^\circ/90^\circ/0^\circ]$)

R/a	Method	[0/90/0]		[0/90/90/0]	
		$a/h = 100$	$a/h = 10$	$a/h = 100$	$a/h = 10$
5	present (13×13)	20.3473	11.5614	20.3824	11.6067
	present (17×17)	20.3389	11.5611	20.3760	11.6064
	present (21×21)	20.3377	11.5611	20.3751	11.6064
	FSDT [55]	20.332	12.207	20.361	12.267
	HSDT [55]	20.330	11.850	20.360	11.830
10	present (13×13)	16.6662	11.5499	16.6778	11.5911
	present (17×17)	16.6634	11.5497	16.6756	11.5909
	present (21×21)	16.6630	11.5497	16.6753	11.5909
	FSDT [55]	16.625	12.173	16.634	12.236
	HSDT [55]	16.620	11.800	16.630	11.790
100	present (13×13)	15.2551	11.5462	15.2536	11.5860
	present (17×17)	15.2518	11.5460	15.2532	11.5858
	present (21×21)	15.2517	11.5460	15.2532	11.5858
	FSDT [55]	15.198	12.163	15.199	12.227
	HSDT [55]	15.19	11.79	15.19	11.78
Plate	present (13×13)	15.2371	11.5461	15.2385	11.5859
	present (17×17)	15.2368	11.5460	15.2382	11.5858
	present (21×21)	15.2368	11.5460	15.2382	11.5858
	FSDT [55]	15.183	12.162	15.184	12.226
	HSDT [55]	15.170	11.790	15.170	11.780

Table 5

Nondimensionalized fundamental frequencies of cross-ply cylindrical shells, $\bar{\omega} = \omega \frac{a^2}{h} \sqrt{\rho/E_2}$